Microsc. Microanal. Microstruct. **8** (1997) 261–272 AUGUST/OCTOBER **1997**, PAGE 261

Characterization of W Films on Si and SiO_2/Si Substrates by X-Ray Diffraction, AFM and Blister Test Adhesion Measurements

Alain Bosseboeuf ([2]), Michel Dupeux ([1]), Mathilde Boutry ([2]), Tarik Bourouina ([2]), Daniel Bouchier ([2]) and Dominique Débarre ([2])

([1]) Laboratoire de Thermodynamique et Physico-Chimie Métallurgiques (CNRS UMR 5614/INPG/UJFG), ENSEEG, BP 75, 38402 Saint-Martin d'Hères, Cedex, France
([2]) Institut d'Électronique Fondamentale (CNRS URA 0022), Université Paris-Sud, Centre d'Orsay, Bâtiment 220, 91405 Orsay Cedex, France

(Received July 28; accepted October 20, 1997)

PACS.68.55.a – Thin film structure and morphology
PACS.68.35.Gy – Mechanical and acoustical properties; adhesion
PACS.81.15.Cd – Deposition by sputtering

Abstract. — Contrary to most classical adhesion test, the blister test provides quantitative adhesion energy measurements. We demonstrate its application to 1 μm thick W films in tensile stress state deposited by xenon DC magnetron sputtering on PECVD/Si(100) substrates. The W films surface morphology, structure and residual stress were also characterized by atomic force microscopy, X-ray diffraction and substrate curvature measurements as function of the deposition pressure. Films characteristics are compared with those of W films deposited directly on Si(100) substrates.

1. Introduction

In a recent review paper [1], Li shows, from a detailed analysis of many published investigations, that a great similarity exists between metal/ceramic interfaces and metal/semiconductor Schottky contacts. This interesting unified picture is based notably on a correlation between works of adhesion of liquid metal/solid oxide systems and barrier heights of metal/semiconductor and metal/insulator interfaces. A direct comparison could not be made for solid metal/solid oxide interfaces because work of adhesion data for such systems are very limited. Indeed, for liquid metals the work of adhesion can be deduced directly from contact angle measurements while most classical adhesion test for thin solid films provide only relative results. The blister test method [2, 3] allows to make quantitative adhesion energy measurements. In addition, the film residual stress and Young's modulus can be evaluated from the initial phase of the test (bulge test). Film stress may be important for a more complete understanding of solid metal/solid substrate interfaces because previous work in one of our laboratory has demonstrated a correlation between W/Si schottky barrier height and W film residual stress [4]. In thin film technology, the blister test method has been mainly used to measure adhesion of

Article available at http://mmm.edpsciences.org or http://dx.doi.org/10.1051/mmm:0199700804-5026100

polymers on inorganic materials or of metals on polymers (see for example [5]). Very few blister test experiments have yet been reported for thin inorganic films on inorganic substrates [6] although bulge test is used for a long time for such systems [7–13]. In this paper we report for the first time on the application of the blister test method to W films deposited by xenon DC magnetron sputtering on Si(100) and on PECVD SiO_2 layers. Beside their theoretical interest, W/Si and W/SiO_2 systems have a practical importance because W films are commonly used in electronic devices for their low resistivity, high thermal stability and fine line patterning ability by dry etching in fluorinated plasmas. To evaluate the morphology, structure, residual stress and the resistivity of the W films deposited on silica, the layers were also characterized by atomic force microscopy (AFM), X-ray diffraction, substrate curvature measurements and four probe measurements. The characteristics of the W films deposited directly on silicon have been reported previously [4, 14] and will only be summarized briefly for comparison with W films deposited on silica.

2. Deposition and Characterization of the Tungsten Films

2.1. Film Deposition

The W films were deposited by DC magnetron sputtering in a commercial reactor on n-Si(100) 2″ wafers covered or not with a 0.15−0.18 nm thick PECVD SiO_2 layer. Just before their introduction in the deposition set-ups, the silicon substrates were chemically cleaned by a standard RCA type procedure followed by an etch of the residual oxide in buffered HF, a short rinsing in desionized water and a filtered N_2 drying. SiO_2 films were deposited at 300 °C from a mixture of SiH_4 (332 sccm) and N_2O (600 sccm). The total pressure and rf low frequency (187 kHz) power were respectively adjusted to 500 mbar and 60 W. For the W films deposition, xenon working gas was used instead of argon because previous work showed that it allows a better residual film stress control [4]. In addition, it leads to twice larger grain sizes and to lower rare gas incorporation and resistivities [4]. All W films were deposited with a DC power of 100 W, a target to substrate distance of 38 mm and a background pressure lower than 2×10^{-4} Pa. The 3 inches in diameter W target used had a nominal purity of 99.95%. The xenon pressure was varied in the range 0.2−2 Pa in order to obtain films with different residual stress state. Contrary to the case of argon, the resulting film deposition rate was found constant within a few % in this pressure range. This means that for xenon the increase of plasma ionization with pressure is compensated by the decrease of ions kinetic energy resulting from the decrease of their mean free path. The deposition rate on SiO_2 was found to have a radial symmetry with a maximum at the center of the wafers equal to about 81 nm/min. Unless otherwise stated the W films investigated have a typical thickness in the range 1−1.2 μm. All films have a xenon content below the detection limit of X-ray micronanalysis in energy dispersive mode ($\leq$ few 0.1‰), a low resistivity ($\leq$ 10 $\mu\Omega$cm) and a low roughness.

2.2. Films Morphology

SEM and AFM observations of W/SiO_2 samples showed a significative change of the surface morphology when the xenon pressure is varied. This is illustrated by the AFM pictures of Figure 1 corresponding to 5×5 μm scans on 1 μm thick W films deposited at various pressures. When the xenon pressure is increased the surface granulosity becomes thinner. The AFM images were analyzed to get the rms roughness from the Gaussian heights distributions and the mean radial spatial period of the roughness from the Fourier transform of the image. Results are plotted in Figure 2 *versus* the xenon deposition pressure. Below about 0.7 Pa the

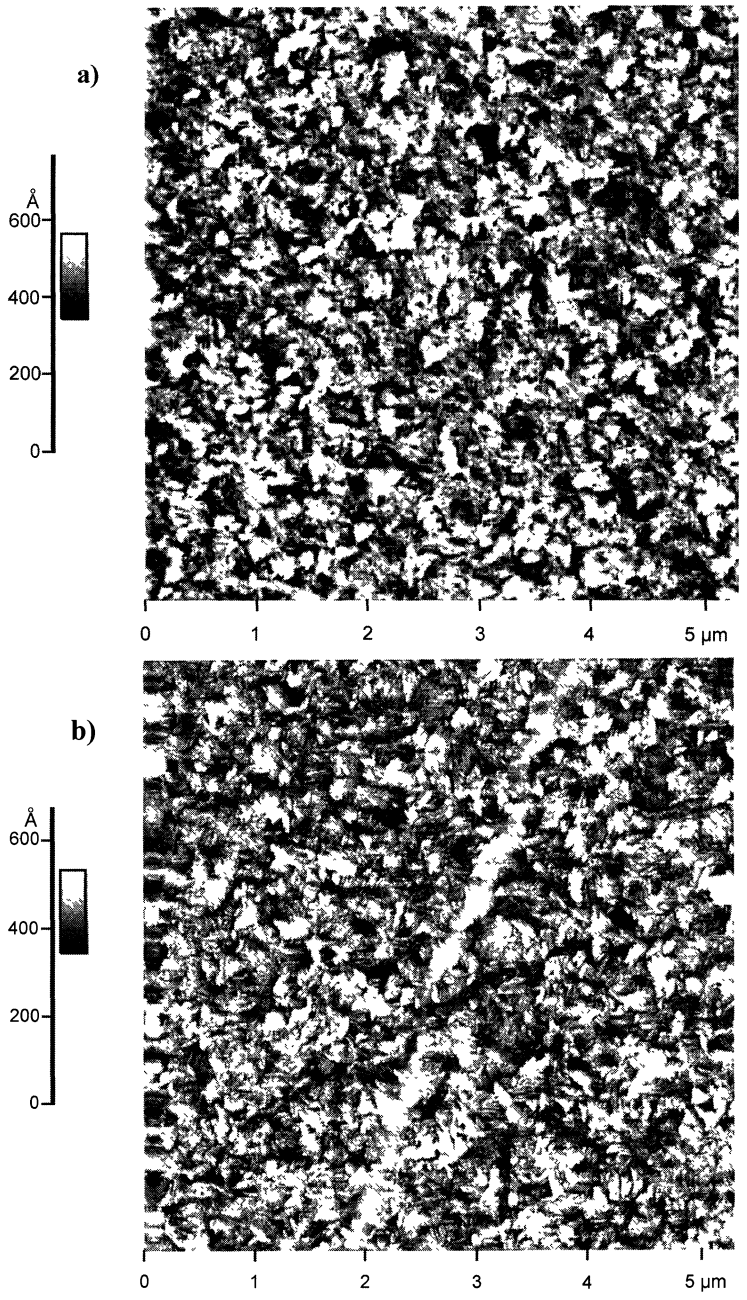

Fig. 1. — Contrast enhanced AFM pictures of W films deposited on PECVD SiO_2 at different xenon pressures: DC power: 100 W. a) $P_{xenon} = 0.39$ Pa, b) $P_{xenon} = 0.7$ Pa, c) $P_{xenon} = 1$ Pa.

spatial period is approximately constant while the roughness slightly decreases. Beyond this pressure, the rms roughness stays constant but the spatial period becomes lower. We will see below (Fig. 7) that the stress state of W films on SiO_2 becomes tensile above this pressure.

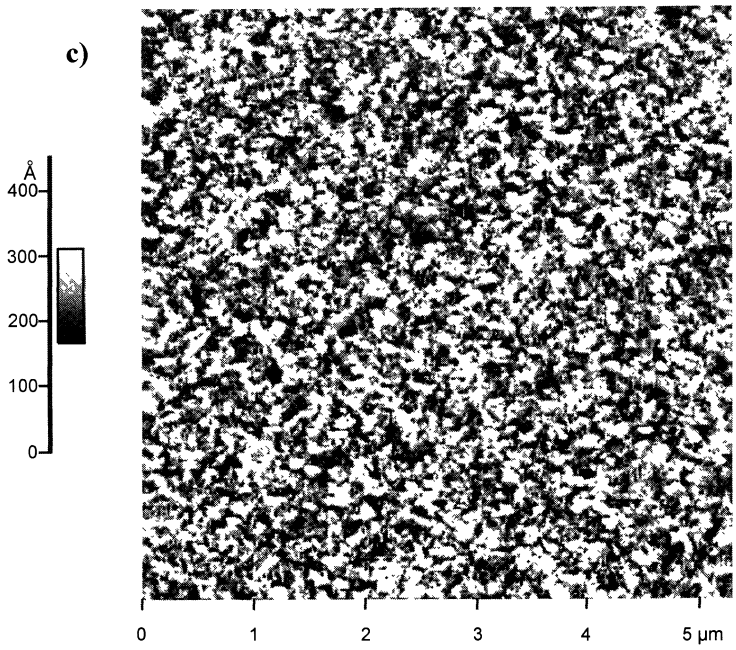

Fig. 1. — (Continued).

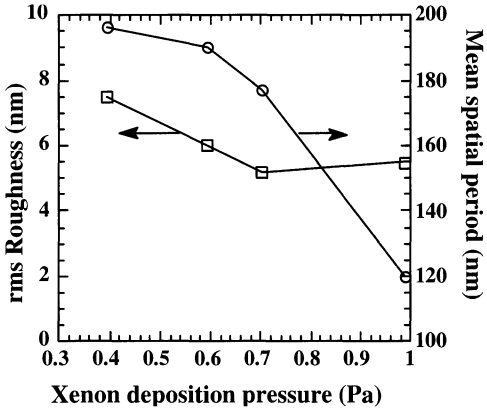

Fig. 2. — RMS roughness and mean radial spatial period of the roughness for 1 μm thick W films deposited on PECVD SiO_2 *versus* xenon deposition pressure.

These results are thought to be related to the variation with pressure of the peening effect [15] *i.e.* the bombardment of the growing film by Xe ions backscattered on the target and sputtered W particles.

2.3. Films Structure

Previous work showed that 0.5 μm thick W films deposited directly on (100) and (111) silicon at 100 W in the same set-up have a bcc α-W structure with a strong (110) preferential orientation

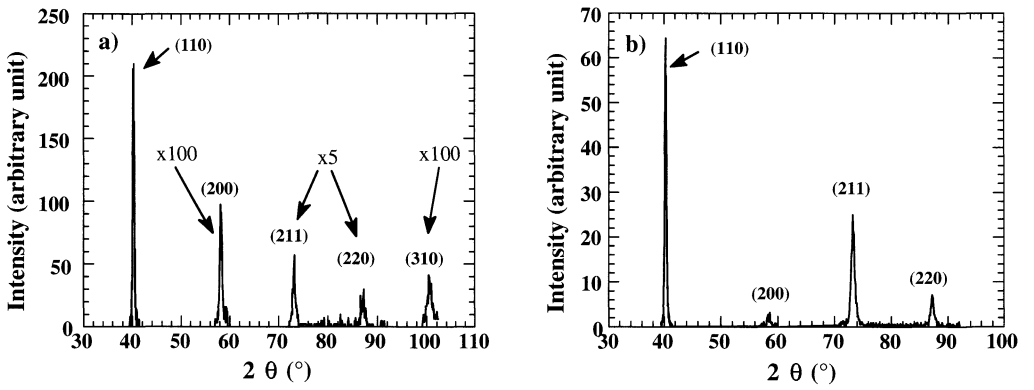

Fig. 3. — X-ray diffraction diagrams of W films deposited on PECVD SiO_2 at different xenon pressure. DC power 100 W. a) $P_{xenon} = 0.2$ Pa, b) $P_{xenon} = 1$ Pa.

whatever the xenon pressure in the range $P = 0.1-4$ Pa [4]. Diffraction coherent domain sizes estimated from the 110 peak were found to be about 50 nm below $P = 2$ Pa and to decrease down to 40 nm beyond [14].

The cristallographic structure of 1 μm thick W films deposited on PECVD SiO_2/Si(100) was characterized for this study with an X-pert Philips diffractometer equipped with a ponctual Cu X-ray source ($\lambda_{K\alpha 12} = 0.1542$ nm) and a graphite monochromator. The Si(400) double peak from the substrate at $\theta_{Ka1} = 34.55°$ and $\theta_{Ka2} = 34.65°$ was used to check the angle calibration and measurement resolution. For xenon pressures in the range 0.2–1 Pa all films display a bcc a-W structure as for films deposited on silicon. The measured lattice parameter is around 0.317 nm in good agrement with the tabulated value (0.3165 nm). However a large change of texture was observed when xenon pressure is varied. This is illustrated by the X-ray diffraction diagrams of Figure 3 corresponding to films deposited at low pressure (0.4 Pa) (Fig. 3a) and high pressure (1 Pa) (Fig. 3b). Note the magnifying factors on the (200), (211), (220) and (310) peaks in Figure 3a. Peaks intensity ratios in Figure 3b are close to tabulated values for polycristalline α-W with a random grain orientation while a (110) preferential orientation is clearly seen for the film deposited at low pressure (Fig. 3a). This texture change is consistent with a larger peening effect at low pressure. Such an increase of preferential orientation with bombardment of the growing film was already observed for DC magnetron sputtered Mo [16] and more generally for various films deposited by other techniques involving ions. An energetic model was proposed recently to account for this effect [17]. This model shows that both the surface energy, the strain energy and the ion stopping energy must be considered. The difference we observed between films deposited on silicon and on silica demonstrates that the effect of the substrate nature should not be underestimated even for relatively thick films.

The diffraction coherent domains sizes were roughly estimated from the peaks FWHM by applying the Debye-Sherrer formula for the (110) plane. The Si(400) substrate peak was used to get an approximate underestimated experimental width. Approximately constant domain sizes around 50 nm were found in the pressure range investigated as for films deposited at low pressure on silicon.

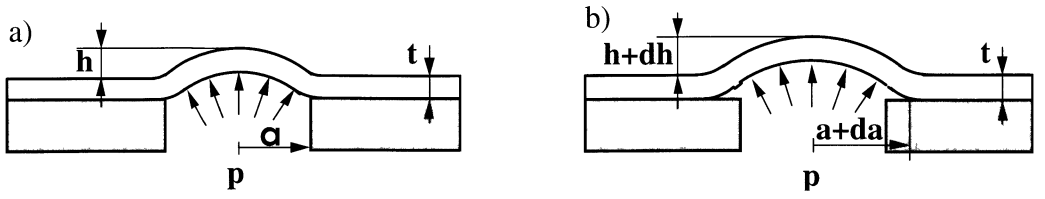

Fig. 4. — a) Bulge test of a thin film bonded to a substrate. b) Blister test: an increase of the applied fluid pressure causes the film to debond from the substrate.

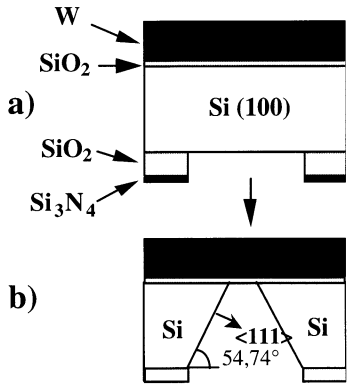

Fig. 5. — Main steps of the W membranes fabrication process. a) Patterning of the masking layers. b) Anisotropic etching of the silicon substrate.

3. Adhesion Measurements by the Blister Test Technique

3.1. The Bulge and Blister Test Technique

In this mechanical test a fluid pressure is applied to one side of a free-standing thin film "window" through a hole in the film substrate [2, 3]. In the first step of the experimental procedure, the fluid pressure causes the film to deflect outwards with an equilibrium shape which can be analyzed on mechanical bases (Fig. 4a). The elastic modulus and the residual stress of the film can be determined from the analysis of this bulge test step. When increasing the fluid pressure, the film may debond from its substrate to form a blister with the shape of a spherical cap (Fig. 4b). The film/substrate adhesion energy can be calculated from an energy balance of the interfacial fracture growth during this blister test step.

Thus both of elastic properties and adhesion energy may be deduced from the same experiment, by increasing the value of the applied pressure. Complete analysis of the results needs a precise knowledge of the specimen dimensions and a continuous monitoring of the blister height *versus* the applied fluid pressure. But a stable mechanical response of the film makes it easier to observe and record the bulged or blistered membrane geometry. This advantage is available even during the interfacial crack propagation, which is intrinsically stable provided that the fluid injection apparatus is rigid enough on itself.

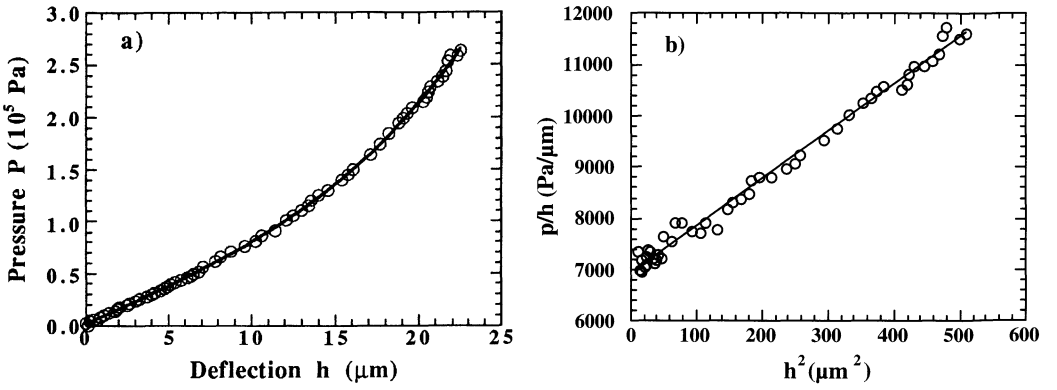

Fig. 6. — Experimental results of the bulge testing of a tungsten film on Si (100) substrate ($t = 1.2$ μm, square window, $2a = 1151$ μm). Deposition conditions: DC power: 100 W, xenon pressure: 1.5 Pa. a) Plot of the applied pressure p *versus* the maximum membrane central deflection h. b) Plot of p/h *versus* h^2.

3.2. Membranes Fabrication Process

Square W membranes with a side length in the range 400−1650 μm and a typical thickness of 1 μm were fabricated for the blister test measurements by a bulk micromachining process (Fig. 5). After W film deposition on the front side of double side polished Si(100) or SiO_2/Si(100) substrates, square patterns were defined by UV lithography and etching in a PECVD Si_3N_4/SiO_2 masking layer deposited at 300 °C on the back side of the wafers (Fig. 5a). Then a 20% KOH solution at 80 °C was used to etch anisotropically square holes in the Si substrate (Fig. 5b). Finally the remaining parts of the masking layers and the optionnal SiO2 layer under the W film were etched in buffered HF. All etching steps were restricted to the wafer back side to avoid W layer degradation.

3.3. Experimental Device

After its preparation the specimen is glued over the central hole of a specimen holder circular plate, which is tightly screwed on the top face of a metal block in which holes connect the specimen to a pressure transducer and to a micrometric screw injection piston. In the present work the inflating fluid is outgassed and distillated water. A stopcock on the block is used to avoid any air bubble formation during the filling of the apparatus, which would cause excessive mechanical compliance of the system.

The whole block size is small enough to allow its positioning on the specimen stage of a metallographic optical microscope equiped with a Michelson interferometric objective and a monochromatic sodium light illumination. After tilt adjustments to compensate for the specimen upper surface inclination, an image of the membrane can be obtained with interference fringes which indicate the iso-altitude lines on the inflated membrane, from which the complete deflected membrane geometry can be deduced.

A CCD camera and a frame grabber are used to digitalize and record the images on a computer, and the analysis and counting of the fringes are made with the help of a image analysis software.

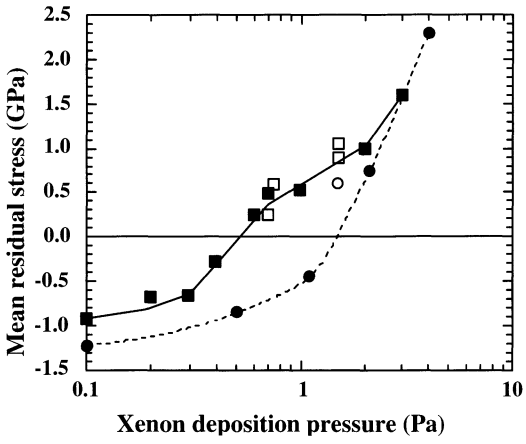

Fig. 7. — Variations of the residual stress in sputtered W films as function of xenon deposition pressure. (●) 0.5 μm thick W films deposited on Si (100); stress measurement by the radius of curvature method [4]. (■) 1 μm thick W films deposited on PECVD SiO_2 underlayer; stress measurement by the radius of curvature method [18]. (○) 1 μm thick deposited on Si (100); stress measurement by the bulge test technique (present work). (□) 1 μm thick W films deposited on PECVD SiO_2 underlayer; stress measurement by the bulge test technique (present work).

3.4. Bulge Test Results

The main experimental result of the bulge test is provided by the plot of the applied pressure p *versus* the maximum deflection of the membrane h in its center (Fig. 6a). The theoretical analysis of the equilibrium shape of the pressurized membrane in bulge test experiments has already been conducted by several authors [3, 9–13] with similar results. With possible refinements, they all converge for large deflections to a description of the pressure *versus* deflection curve in terms of the following polynomial equation :

$$p = c_1 \frac{\sigma_0}{a^2} h + c_2 \frac{Mt}{a^4} h^3 \tag{1}$$

in which σ_0 is the residual equi-biaxial stress in the film, $M = E/(1-\nu)$ is the in-plane biaxial elastic modulus of the film, t is the film thickness. For a circular membrane, a is the membrane radius; for a square membrane, $2a$ is the membrane edge length. c_1 and c_2 are two numerical constants which depend on the shape and thickness-to-size ratio of the membrane and which are adjusted with help of F.E.M. numerical simulations of the membrane behaviour.

A linear fit of the experimental data plotted under the form of p/h *versus* h^2, as it is shown in Figure 6b, then leads to the values of σ_0 and M in the film. In our case we used the numerical values of c_1 and c_2 suggested by Nix *et al.* [3] to calculate the film residual stresses and biaxial moduli. The values of the mean residual stresses are indicated in Figure 7 and compared to values obtained previously by the substrate curvature method as functions of xenon deposition pressure [4, 18]. It can be seen that both kinds of results are consistent for films in tensile stress state, which confirms the reliability of the bulge test as a residual stress determination method when buckling of the membrane does not occur. Results from substrate curvature measurements show a monotonic transition from a compressive stress state at low pressure to a tensile stress state above a critical rare gas pressure. As discussed previously for W/Si samples [4], this behaviour mainly results from peening effect during deposition. The critical

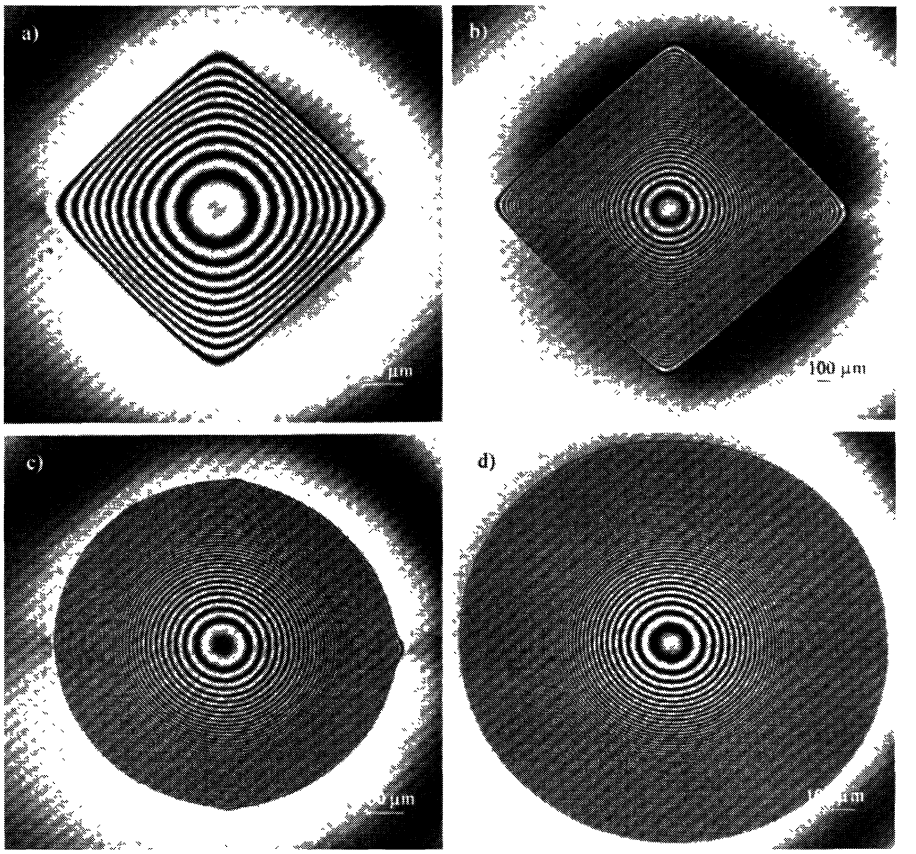

Fig. 8. — Blister test sequence during debonding of a tungsten film on SiO_2/Si substrate; the interference fringe altitude separation is 0.29 μm. sputtered W film: DC power: 100 W, $P_{xenon} = 0.7$ Pa, thickness 1.2 μm. Initial square window, 670.5 μm edge length. PECVD SiO_2 underlayer (300 °C), thickness 150 nm. Si (100) substrate, thickness 290 μm. a) Bulging: $p = 2.76 \times 10^5$ Pa; b) bulging: $p = 1.72 \times 10^5$ Pa; c) partial debonding: $p = 1.08 \times 10^5$ Pa; d) total debonding: $p = 1.37 \times 10^5$ Pa.

xenon pressures and curves shapes are notably different for 1 μm thick films deposited on SiO_2 and for 0.5 μm films deposited on Si. Complementary work would be needed to determine if this is related to in-depth stress gradients which are common in metallic films [19] or to the difference of texture between these films.

The elastic moduli of the tungsten films which have been deduced from our bulge test experiments are also consistent with the common values in literature for bulk tungsten, but the precision of the results is less satisfactory. Actually, the slope of the linear fit of experimental data as in Figure 6b is less precisely determined than the intercept mostly because of incertitude on the membrane geometry, as discussed by Small *et al.* [11].

3.5. Blister Test Results

When increasing the fluid injected volume, a transition occurs in the increasing pressure regime when the film starts to debond from the substrate. This debonding starts from the middle of the four edges of the square window and propagates until the interfacial crack front becomes

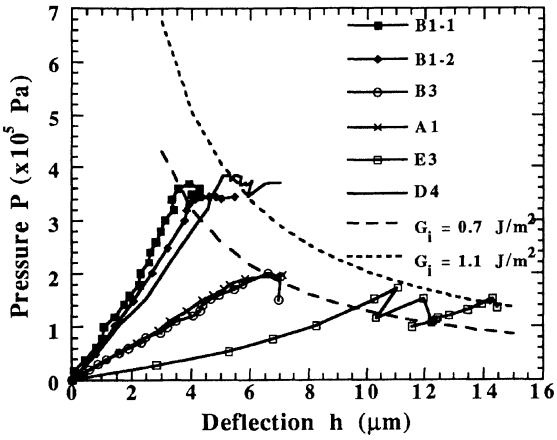

Fig. 9. — Summary of bulge and blister curves for $W/SiO_2/Si$ specimens Specimens A1, B1-1, B1-2, B3 on one hand, E3 and D4 on the other hand, belong to two separate deposition runs. Debonding theoretical hyperbolic curves for $G_i = 0.7$ J/m^2 and $G_i = 1.1$ J/m^2 are plotted in dashed lines.

fully circular, as can be seen on the images of Figure 8. During this debonding, the increase in height and diameter of the blister induces a relaxation of the fluid pressure.

The value of the crack propagation energy release rate can be calculated by writing that the work done by the pressurized fluid during the blister growth is converted into elastic energy stored in the membrane plus new interfacial fracture surfaces [5,20]. This results in the following blister equation :

$$Cph = G_i \tag{2}$$

where G_i is the interfacial adhesion energy. C is a dimensionless parameter which depends on the variable $\zeta = (M/\sigma_0)(h/r)^2$ [5] where r is the blister radius and other symbols were defined above. The theoretical value of C increases only by 25% when ζ varies from 0 to infinity [5]. In our case ζ is always ≤ 0.2 and a value of C equal to 0.54 was taken for all samples. The relationship between p and h in the debonding regime is thus approximately an hyperbolic curve the position of which is intrinsically significant of the adhesive strength of the investigated interfaces.

Figure 9 summarizes the bulge and blister curves which have been obtained so far on various $W/SiO_2/Si$ specimens. The transition points between the bulge regime and the debonding regime are clearly observable, though the blister growth regime is either very short — due to anticipated brittle membrane rupture — or serrated and oscillating — due to excessive compliance of the injection device. However, all the transition points and blister growth regimes seem to lie between the debonding theoretical hyperbolic curves corresponding to adhesion energy between 0.7 and 1.1 J/m^2. It must also be pointed out that the W films of specimens labelled B1-1, B1-2, A1 and B3, which stay mostly on the lower limit of the debonding curve interval, have been deposited in a different run from specimens D4 and E3, which seem to be closer to the upper limit of the adhesion energy range. These runs were performed several monthes apart after a complete maintenance operation on the PECVD set-up and after the installation of a new W target on the sputtering set-up. No change of the SiO_2 and W films characteristics could be evidenced except a slight improvement of the W film resistivity. The blister test results show that this adhesion test method can be sensitive enough to detect slight variations of the interface processing conditions.

No obvious indication of residual stress influence on the adhesion energy could be deduced from these results. For instance, specimens D4 ($\sigma_0 = 0.65$ GPa) and E3 ($\sigma_0 = 0.24$ GPa) are consistent with similar values of adhesion energy close to 1.1 J/m^2.

No debonding could be obtained on the W/Si specimens before bursting out of the membranes, which occured for a pressure value corresponding to a theoretical debonding curve with $G_i = 3.2$ J/m^2. This indicates much better adhesive strength for W/Si interfaces than for W/SiO_2/Si. This qualitative indication has been confirmed by cyclic micro-scratch tests [21] conducted on the same specimens, with specimens D4 and E3 standing 5 to 20 scratch cycles before debonding, while our W/Si specimens stood for more than 50 scratch cycles without damaging.

Results for W/Si samples are only in qualitative agreement with the "universal" Schottky barrier height *versus* work of adhesion curve of Li [1] as the measured Schottky barrier height is about 0.56 eV [4] while the Li curve would predict a value close to 0.4 eV.

4. Conclusion

Polycristalline α-W films with low roughnesses and resistivities have been deposited by xenon DC magnetron sputtering on SiO_2/Si and Si(100) substrates. The morphology, texture and residual stress of the films are variable with deposition pressure according to the peening effect. The possibility of adhesion measurements by the blister test method on micromachined 1m thick square W membranes have been demonstrated. The results show that the adhesion energy of W/SiO_2 is low and in the range 0.7–1.1 J/m^2 according to sample preparation. In the limit of the accuracy of the results, the adhesion energy seems independent of the residual stress in the film. The adhesion energy of W/Si is larger (≥ 3.2 J/m^2) in agreement with cyclic microscratch test measurements but could not be measured exactly because of film breaking before debonding. In both cases stress values deduced from the bulge phase are in fair agreement with stress values obtained by substrate curvature measurements. Special sample preparation are needed to allow larger adhesion energy measurements by the blister test technique on such thin films.

Acknowledgments

The authors are grateful to the French "Centre National de la Recherche Scientifique" and to the members of the G.D.R. "Caractérisation des Interfaces dans les Multi-Matériaux" for their scientific and financial support.

References

[1] Li J.-G., *Mat. Chem. Phys.* **47** (1997) 126-145.
[2] Jensen H.M., *Eng. Fract. Mech.* **40** (1991) 475-486.
[3] Hohlfelder R.J., Vlassak J.J., Nix W.D., Luo H. and Chidsey C.E.D., *Mat. Res. Soc. Symp. Proc.* **356** (1995) 585-590.
[4] Mamor M., Dufour-Gergam M., Finkman L., Tremblay G., Meyer F. and Bouziane K., *Appl. Surf. Sci.* **91** (1995) 342-346.
[5] Hohlfelder R.J., Luo H., Vlassak J.J., Chidsey C.E.D. and Nix W.D., *Mat. Res. Soc. Symp. Proc.* **436** (1997) 115-120.

[6] Sizemore J.T., Hohlfelder R.J., Vlassak J.J. and Nix W.D., *Mat. Res. Soc. Symp. Proc.* **383** (1995) 197-207.
[7] Bromley E.I., Randall J.N., Flanders D.C. and Mountain R.W., *J. Vac. Sci. Technol. B* **1** (1983) 1364-1366.
[8] Allen M.G., Mehregany M., Howe R.T. and Senturia D., *Appl. Phys. Lett.* **51** (1987) 241-243.
[9] Bonnotte E., Delobelle P., Bornier L., Trollard B. and Tribillon G., *J. Phys. III France* **5** (1995) 953-983.
[10] Tabata O., Kawahata K., Sugiyama S. and Igarashi I., *Sensors Actuators A* **20** (1989) 135-141.
[11] Small M.K., Vlassak J.J., Powell S.F., Daniels B.J. and Nix W.D., *Mat. Res. Soc. Symp. Proc.* **308** (1993) 159-164.
[12] Paviot V.M., Vlassak J.J. and Nix W.D., *Mat. Res. Soc. Symp. Proc.* **356** (1995) 579-584.
[13] Maier-Schneider D., Maibach J. and Obermeier E., *J. Microelectromech. Syst.* **4** (1995) 238-241.
[14] Mamor M., Étude de diodes Schottky tungstène sur des alliages SiGeC élaborés par RTCVD, Doctorate thesis, University Paris XI, Orsay (1996).
[15] Carter G., *J. Phys. D. Appl. Phys.* **27** (1994) 1046-1055.
[16] Zaouli M., Lebrun J.L. and Gergaud P., *Surf. Coatings Techn.* **50** (1991) 5-10.
[17] Zhao J.P., Wang W., Chen Z.Y., Chang S.Q., Shi T.S. and Liu X.Y., *J. Phys. D: Appl. Phys.* **30** (1997) 5-12.
[18] Boutry M., Étude de microdispositifs de test pour la caractérisation des propriétés mécaniques de films minces métalliques, Doctorate Thesis, Université Paris XI, Orsay (1997).
[19] Boutry M., Bosseboeuf A. and Coffignal G., Characterization of residual stress in metallic films on silicon with micromechanical devices, Proc. SPIE-Micromachining and microfabrication, Austin (USA) (1996) pp. 126-134.
[20] Sizemore J., Stevenson D.A. and Stringer J., *Mat. Res. Soc. Symp. Proc.* **308** (1993) 165-170.
[21] Consiglio R., Von Stebut J. and Badawi K., poster communication, national meeting "Interfaces et Multi-Matériaux" (I2M), C.N.R.S.- E.N.S.A.M., Aix-en-Provence (France) May 26-28, 1997.